

## Deriving Kinetic Insights from Mechanochemically Synthesized Compounds Using Multivariate Analysis (MCR-ALS) of Powder X-Ray Diffraction Data

Laura Macchietti,<sup>a</sup> Lucia Casali,<sup>a,b</sup> Franziska Emmerling<sup>b,\*</sup> Dario Braga, and Fabrizia Grepioni<sup>a,\*</sup>

### Electronic Supplementary Information (16 pages)

#### 1. Table ESI 1. Single crystal data at room temperature

	TP·MA monoclinic (CC-M)	TP·MA triclinic (CC-T)
Formula	C10 H12 N4 O6	C10 H12 N4 O6
fw	284.24	284.24
Cryst. System	monoclinic	triclinic
space group	C2/c	P -1
Z, Z'	8, 1	4, 2
a (Å)	17.2266(11)	8.1438(6)
b (Å)	8.3825(4)	12.4857(10)
c (Å)	17.7760(11)	12.9437(10)
$\alpha$ (deg)	90	92.848(6)
$\beta$ (deg)	104.365(7)	103.379(6)
$\gamma$ (deg)	90	102.355(7)
V (Å <sup>3</sup> )	2486.6(3)	1243.92(17)
D <sub>calc</sub> (g/cm <sup>3</sup> )	1.518	1.518
$\mu$ (mm <sup>-1</sup> )	0.13	0.13
Measd reflns	5748	10235
Indep reflns	2856	5652
R1 [on F <sub>o</sub> <sup>2</sup> , I > 2 $\sigma$ (I)]	0.0634	0.0684
wR2 (all data)	0.1477	0.1505

Deposition Numbers in the CSD database: CC-T: 2305331; CC-M: 2305332

#### 2. Quantitative analysis of ex situ data by Rietveld Method

The comparison between the quantitative results from the MCR-ALS and the phase quantification via Rietveld analysis reported in section 3.2, presented a good agreement between the two calculation methods. Looking at the values obtained for the Rietveld quantification of theophylline and malonic acid (Table 1), the two reagents differ to up 8 percentage points between all the experiments, while the mixture contains equimolar concentration, and the stoichiometry of both co-crystal forms is 1:1, thus we expected an equal amount of both compounds being consumed. The graphs in Figure ESI 1 plot the difference between the TP and MA values of the Rietveld analysis against the difference registered between the two methods, for each component. There is a correlation in the data of both reagents and CC-T, for which the increase in the gap

between the two starting materials quantification sees an increase in the discrepancy between the methods results. The CC-M results, instead, associated with the lowest methods gap and randomly distributed errors, show no correlation. The presence of a systematic bias on the quantification of the reagents and the CC-T phases, might be due to different effect affecting the Rietveld calculation, including the presence of preferred orientation that we tried to investigate. The preferred orientation was first observed on the diffractogram of the pure malonic acid, and the output of the Rietveld analysis (Figure ESI 2 and Figure ESI 3) also presented an evident discrepancy between the calculated profile and the experimental pattern at around  $23.5^\circ 2\theta$  (orange rectangle), matching the malonic acid peak involved in the phenomenon. Therefore it was attempted to improve the Rietveld modelling of the preferred orientation with the introduction of spherical harmonics showed that, while the correction improved the fitting of the profile, the gap between the reagents and the methods was not significantly reduced, therefore the correction was not applied. The final fitting returned a mean value of the RWP, between all the eleven acquisitions of 9.6.

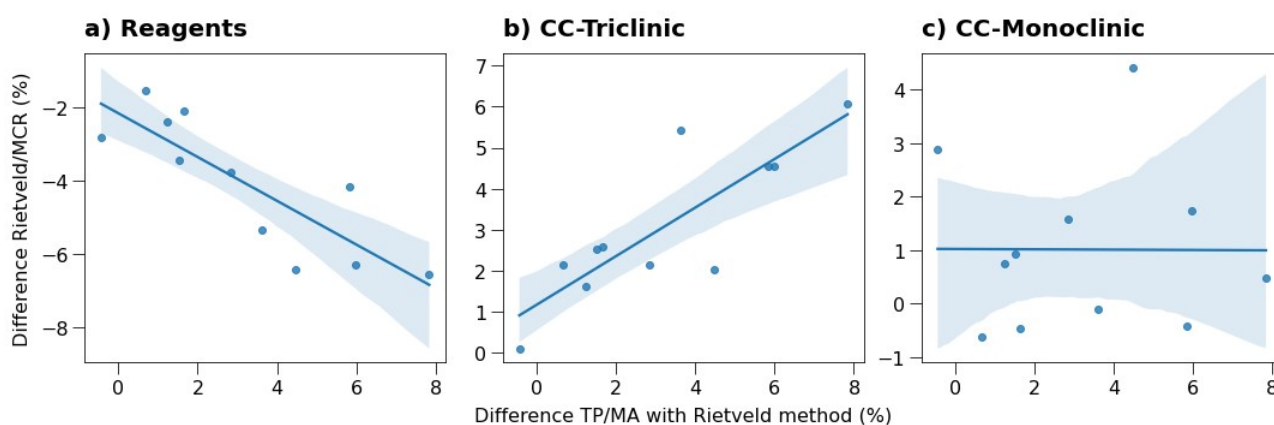


Figure ESI 1 - Scatterplots plotting on the x axis the difference in quantification of the two reagents (theophylline and malonic acid) from the Rietveld method (ex situ data), against the difference between the two model results (y-axis). Each plot reports on the y-axis the difference of a specific component (a: reagents, b: CC-T, c: CC-M). The line visualizes a linear regression fitted on the data to highlight possible correlations between the plotted variables.

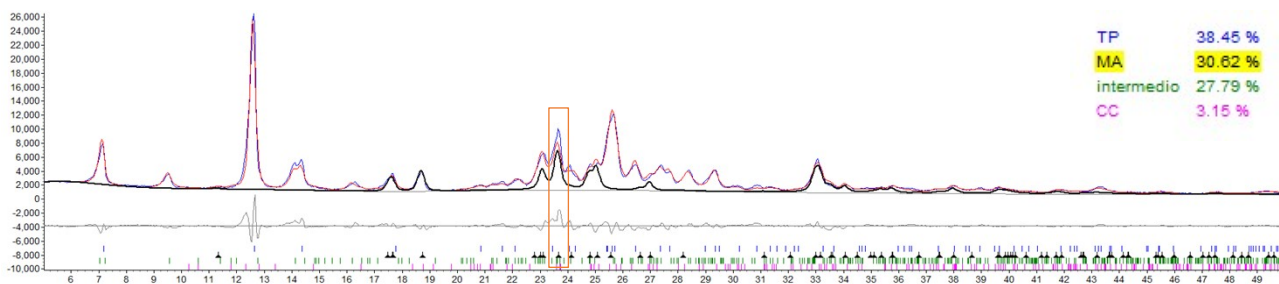


Figure ESI 2 - Rietveld mixture analysis on the t0 acquisition of the ex situ experiment: the sum of all the calculated phases is shown in red, the diffraction pattern in blue, the difference plot in grey. The black line shows the fitted profile of the malonic acid (MA) component.

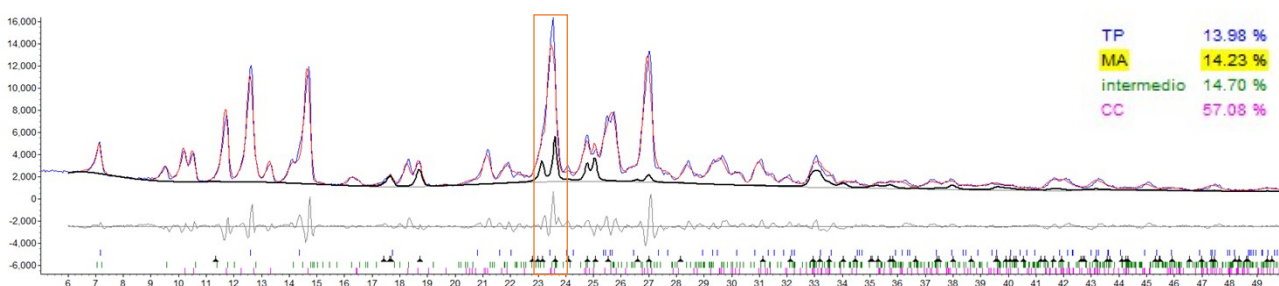


Figure ESI 3 - Rietveld mixture analysis on the 20h acquisition of the ex situ experiment: the sum of all the calculated phases is shown in red, the diffraction pattern in blue, the difference plot in grey. The black line shows the fitted profile of the malonic acid (MA) component.

Table ESI 2 - Results of the Rietveld phase quantification on the ex situ data set

	Theophylline (%)	Malonic Acid (%)	CC-T (%)	CC-M (%)
<b>t0</b>	38.5	30.6	27.8	3.1
<b>30min</b>	32.9	27.0	35.9	4.2
<b>1h</b>	29.1	23.1	39.5	8.3
<b>1.5h</b>	24.8	23.3	40.5	11.4
<b>2h</b>	23.8	22.2	41.4	12.7
<b>3h</b>	22.3	18.7	41.4	17.6
<b>4h</b>	20.6	19.9	37.5	22.0
<b>20h</b>	14.0	14.4	14.7	57.1
<b>24h</b>	13.9	11.0	8.9	66.2
<b>28h</b>	13.3	8.8	7.4	70.5
<b>45h</b>	10.3	9.1	4.4	76.2

### 3. Pure profiles resulting from the MCR-ALS calculation on in situ data: NG experiments.

H1: comparison with reference pattern

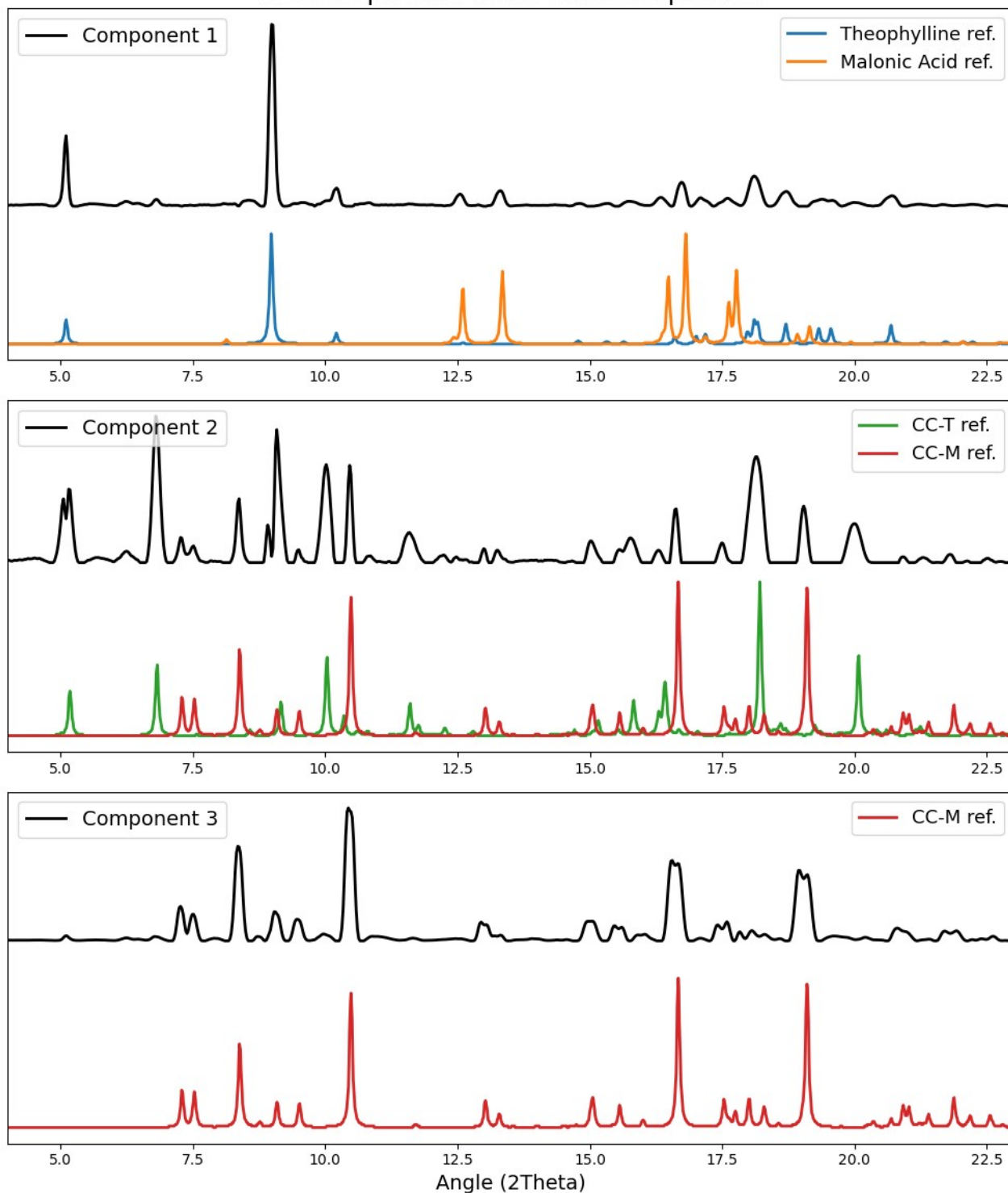


Figure ESI 4 - Comparison of the pure profiles (S matrix, black lines), resulted for the MCR-ALS calculation on the H1 (50 Hz) data, with the reference patterns (coloured lines).

## H2: comparison with reference pattern

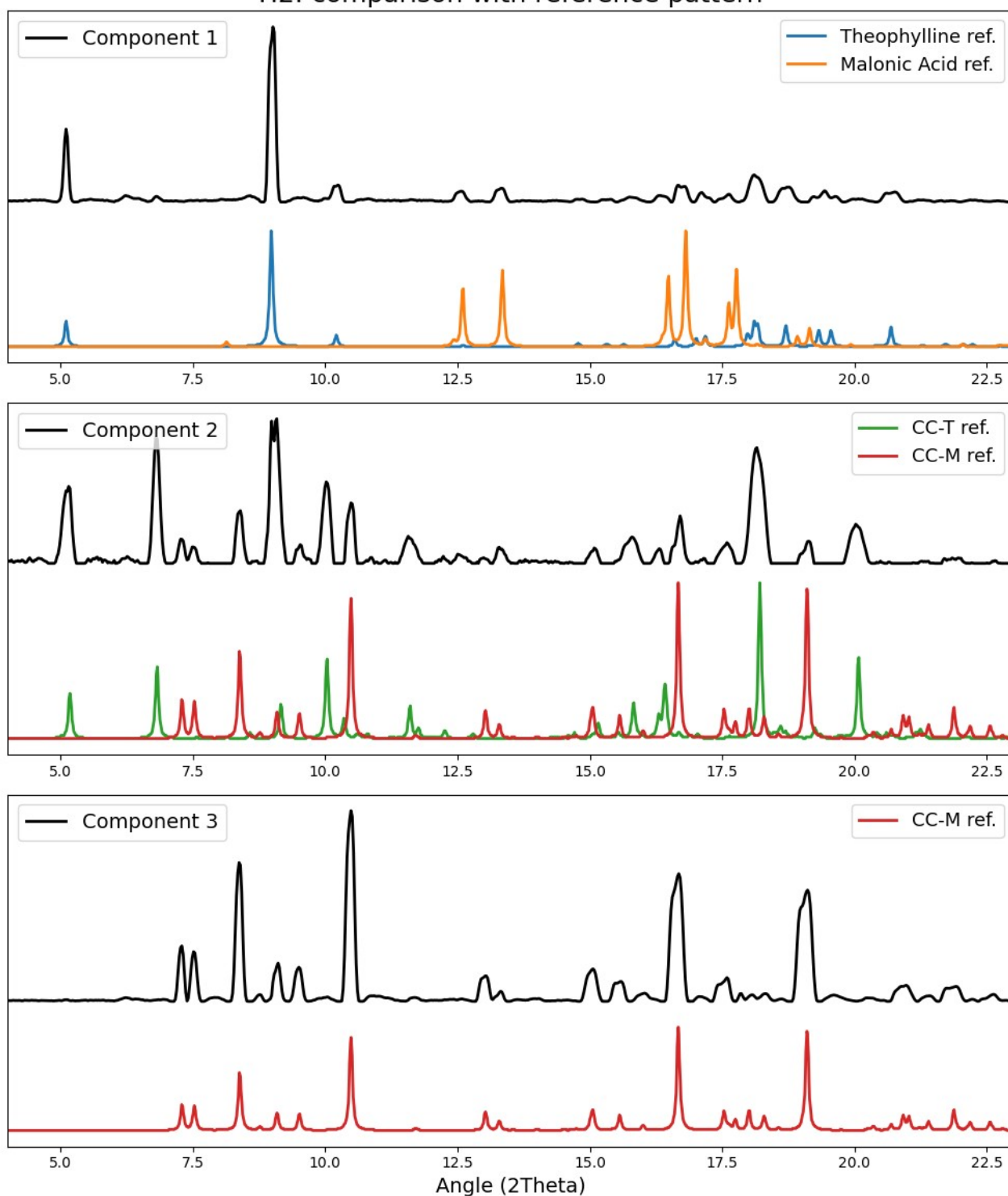


Figure ESI 5 - Comparison of the pure profiles (S matrix, black lines), resulted for the MCR-ALS calculation on the H2 (50 Hz) data, with the reference patterns (coloured lines).

### L1: comparison with reference pattern

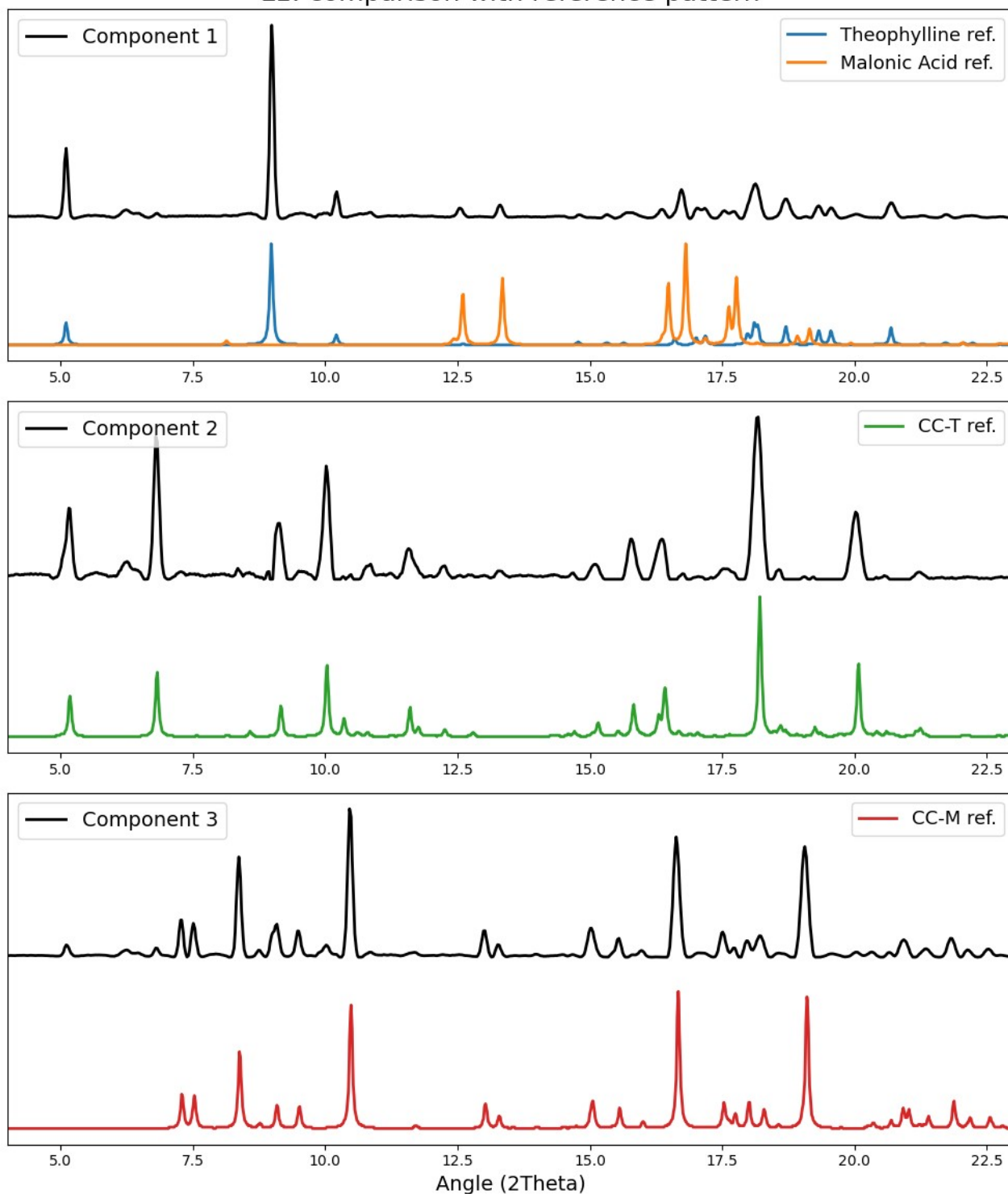


Figure ESI 6 - Comparison of the pure profiles (S matrix, black lines) resulted for the MCR-ALS calculation on the L1 (25 Hz) data, with the reference patterns (coloured lines).

### T50: comparison with reference pattern

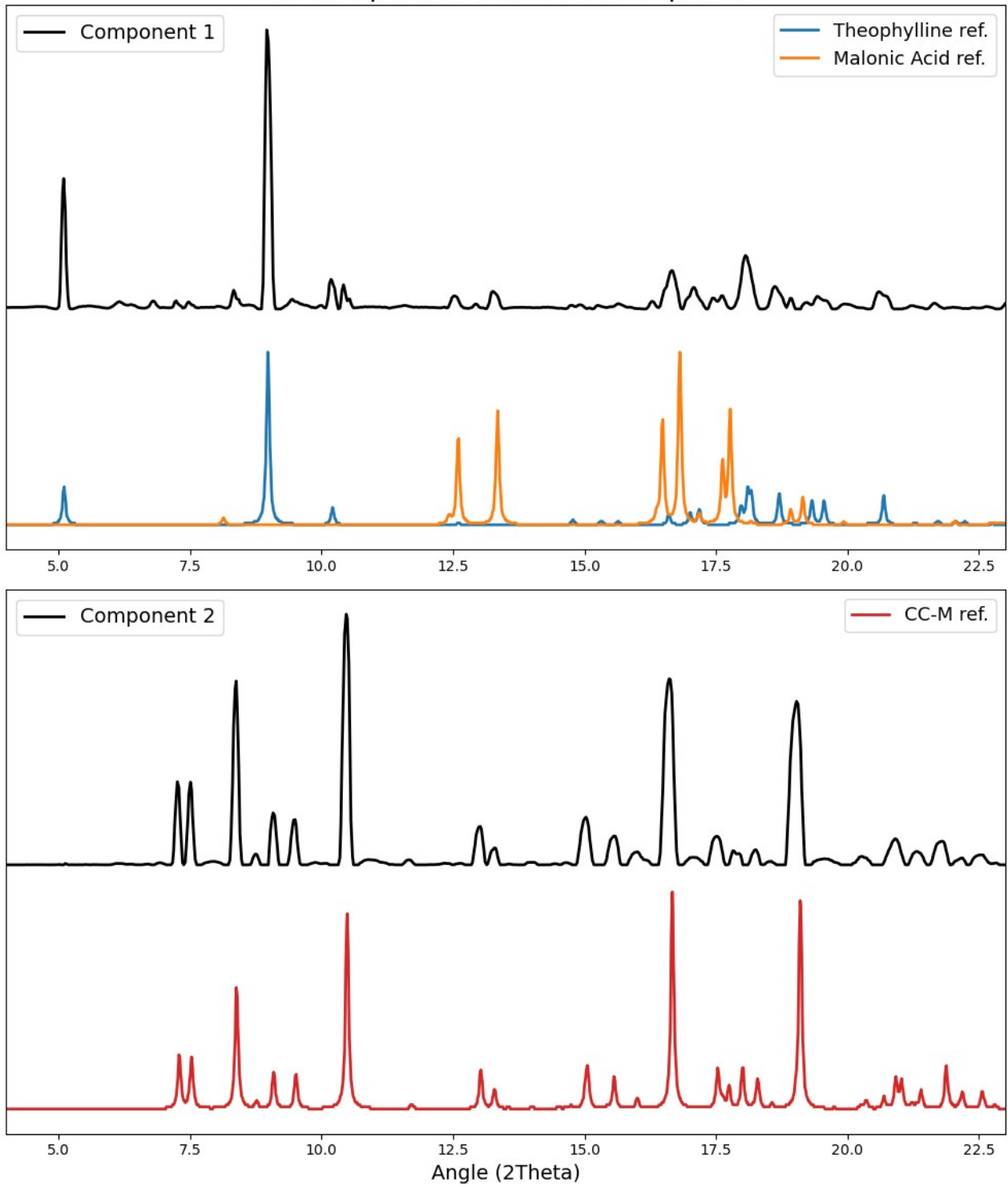


Figure ESI 7 - Comparison of the pure profiles (S matrix, black lines) resulted for the MCR-ALS calculation on the T50 (25 Hz, 50 °C) data, with the reference patterns (coloured lines).

### T80: comparison with reference pattern

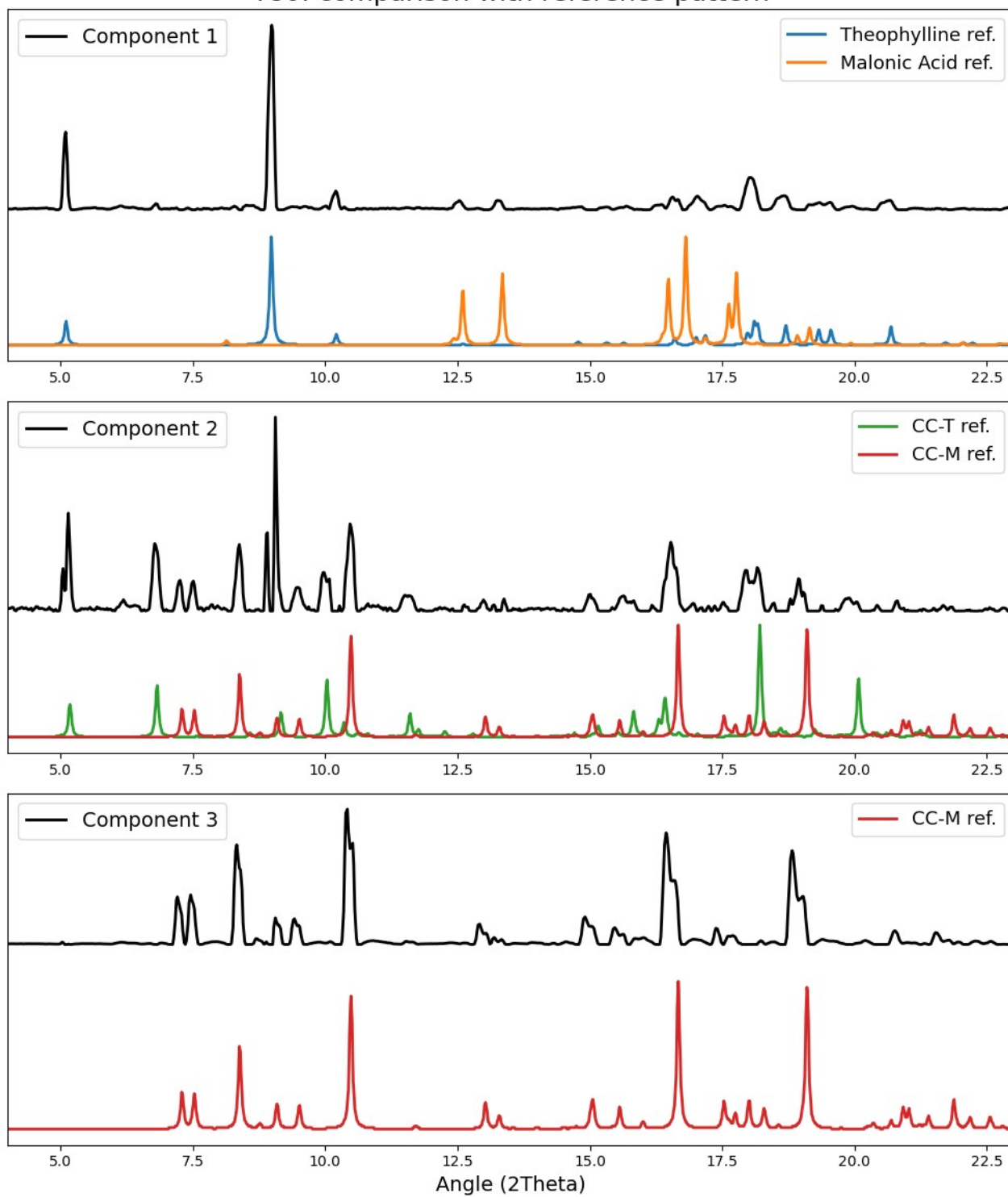


Figure ESI 8 - Comparison of the pure profiles (S matrix, black lines) resulted for the MCR-ALS calculation on the T80 (25 Hz, 80 °C) data, with the reference patterns (coloured lines).

4. Pure profiles resulting from the MCR-ALS calculation on in situ data: LAG experiments.

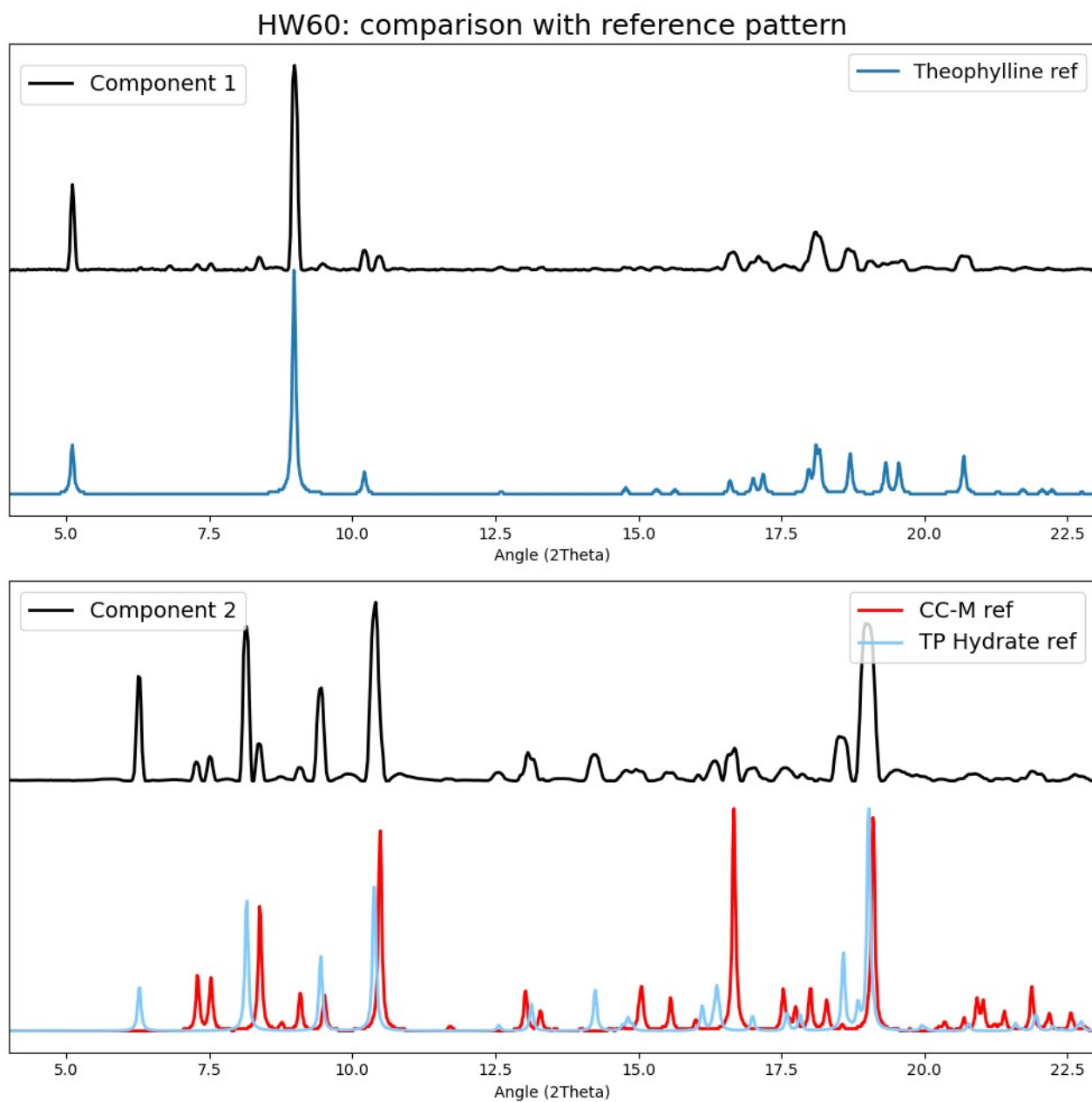


Figure ESI 9 - Comparison of the pure profiles (S matrix, black lines) resulted for the MCR-ALS calculation on the HW60 (50 Hz, 60  $\mu$ L) data, with the reference patterns (dotted lines).

### HW30: comparison with reference pattern

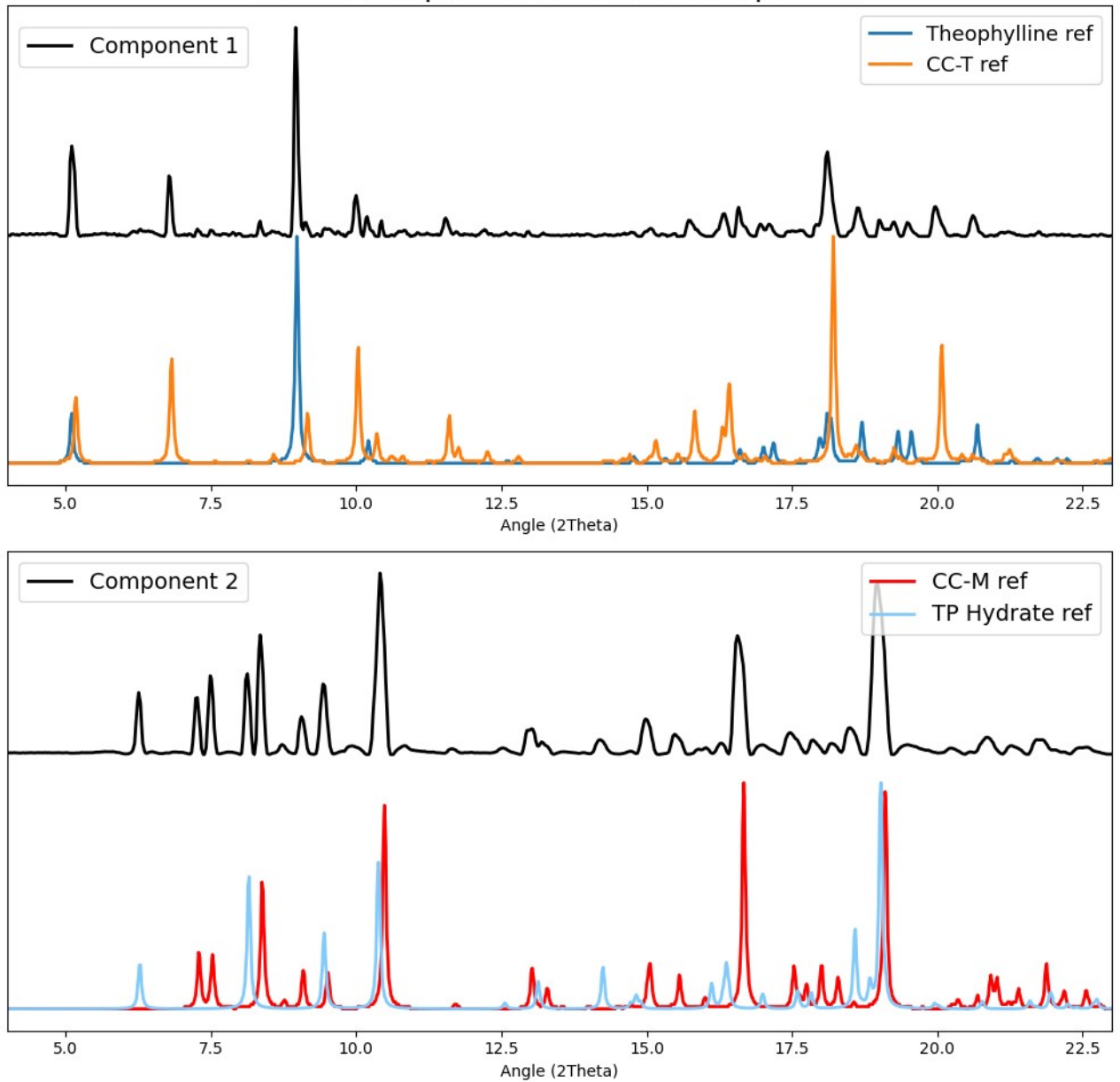


Figure ESI 10 - Comparison of the pure profiles (S matrix, black lines), resulted for the MCR-ALS calculation on the T50 (25 Hz, 50 °C) data, with the reference patterns (dotted lines).

### LW30: comparison with reference pattern

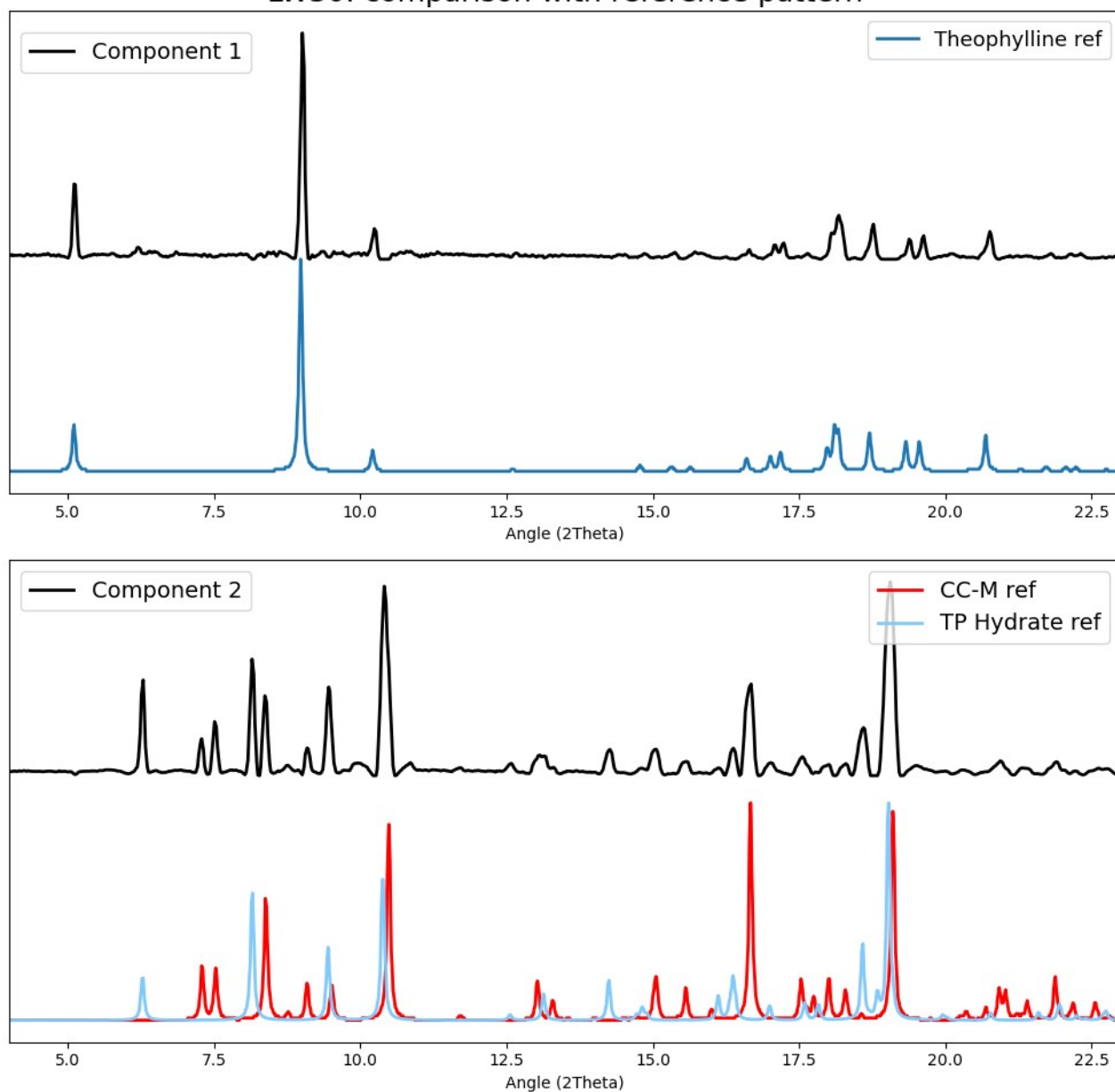


Figure ESI 11 - Comparison of the pure profiles (S matrix, black lines) resulted for the MCR-ALS calculation on the LW30 (25 Hz, 30  $\mu$ L) data, with the reference patterns (dotted lines).

### LW10: comparison with reference pattern

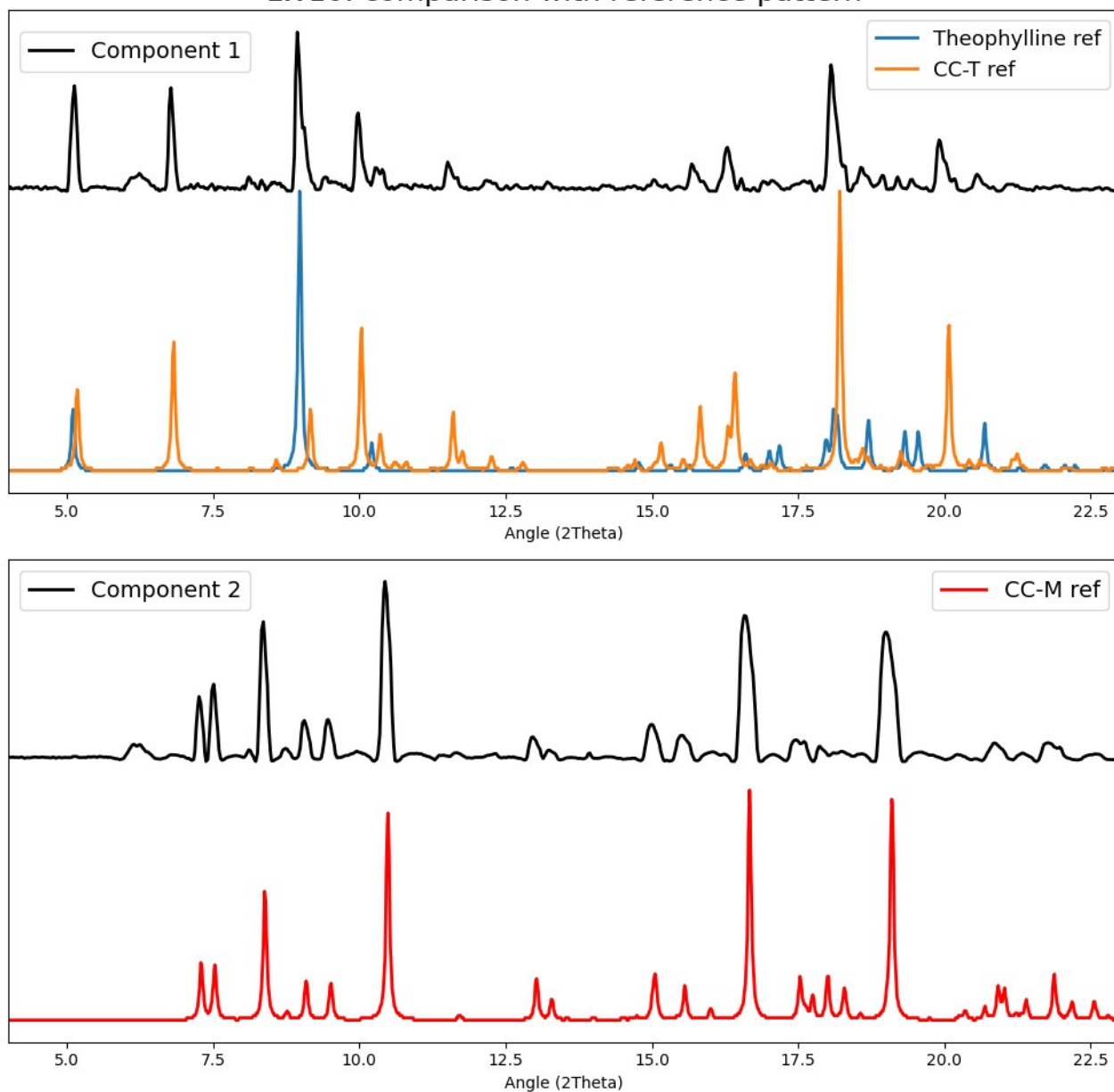


Figure ESI 12 - Comparison of the pure profiles (S matrix, black lines) resulted for the MCR-ALS calculation on the LW30 (25 Hz, 30  $\mu$ L) data LW10 (25 Hz, 10  $\mu$ L), with the reference patterns (dotted lines).

## 5. Comparison between MCR concentration profiles and characteristic peaks evolution on experimental powder XRD data.

The series of plots in Figure ESI 13 displays the concentration curves returned by the MCR calculation for the two 50 Hz tests (RT in NG condition), of both co-crystal polymorphs, on top of the detail of a characteristic diffraction peak of the respective phase observed on the experimental data for each test. The experimental data is shown at selected time acquisitions allowing to follow the evolution of the phases and to compare the kinetics with the results of the model. The times of appearance/disappearance and the relative intensities of the peaks from the experimental data agree with the profile obtained with the MCR-ALS method, confirming the variability of the transformation in the specific tested conditions.

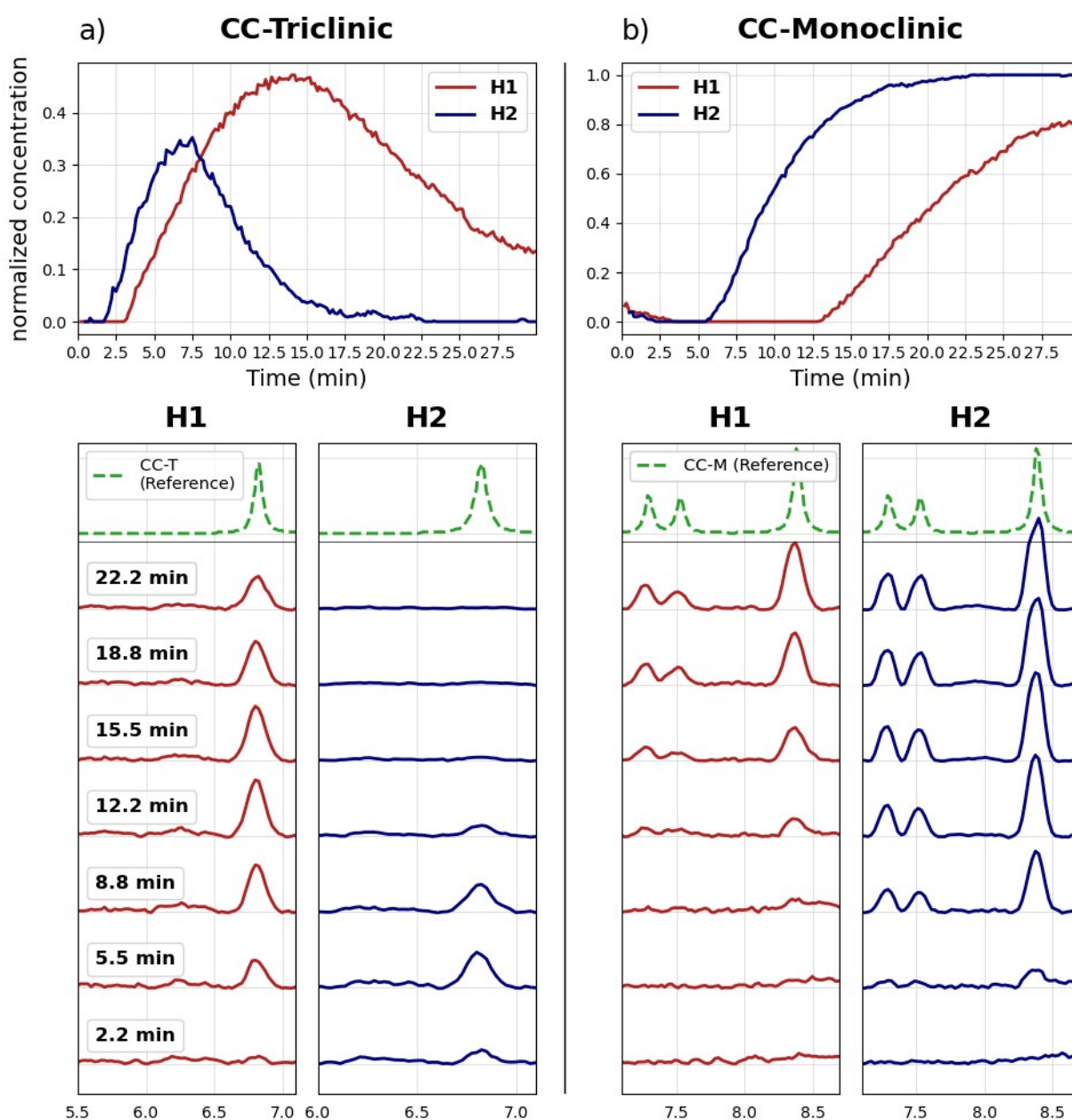


Figure ESI 13 – Analysis of the kinetics of CC-T (a) and CC-M (b) formation in the H1 and H2 tests, comparing the MCR-ALS concentration profiles (top graph), and the experimental diffractograms (lower graphs, H1: red, H2: blue). The selected time points for the experimental data are the same for both tests and phases, labels are then reported only once on the first plot on left (CC-T/H1). In green dotted line are reported the calculated patterns of the respective phases, as reference for the characteristic peaks shown.

## 6. Detail from test T50 experimental PXRD data

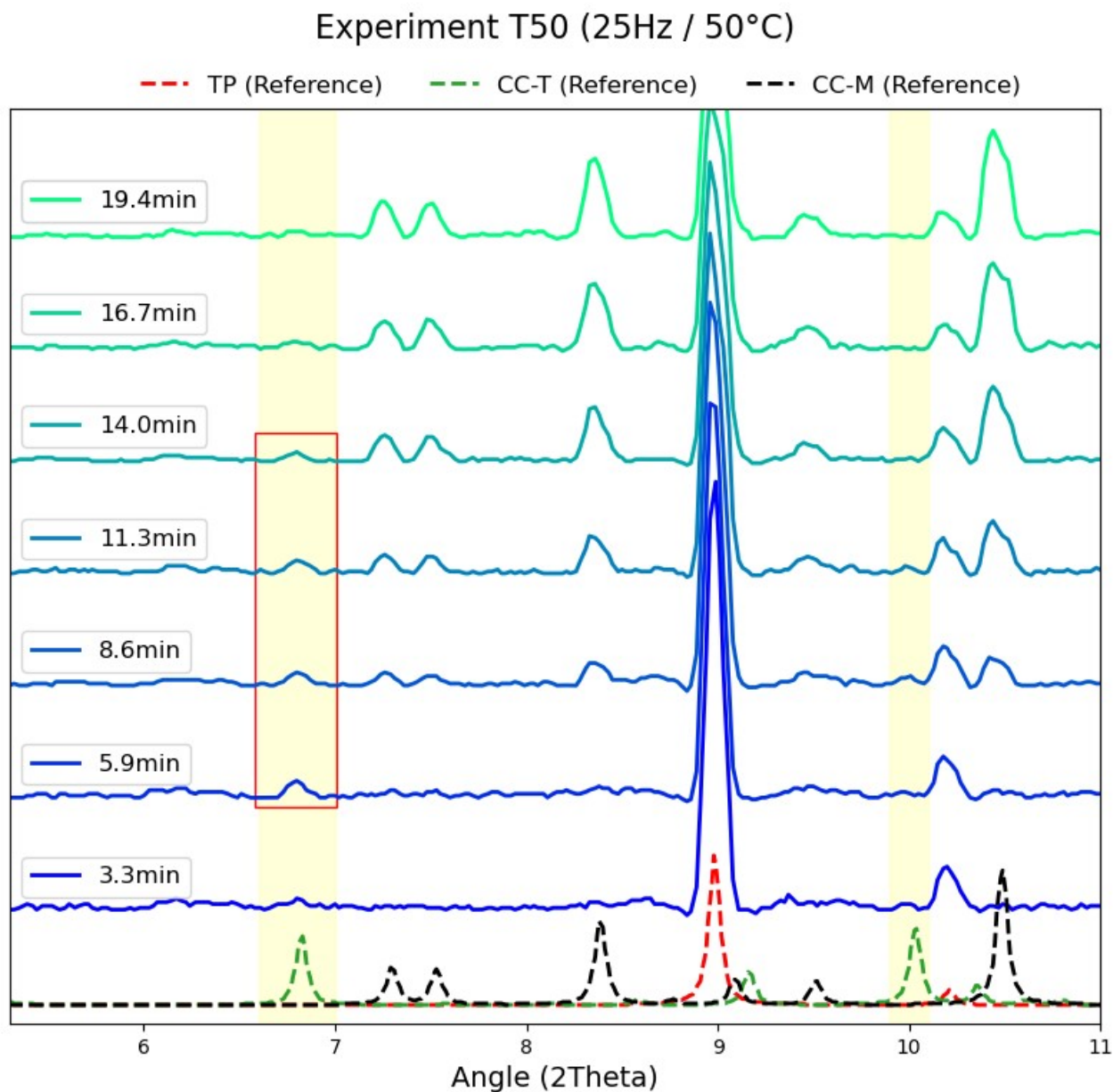


Figure ESI 14 - Experimental patterns for the 50°C test registered in situ between 3 and 19 min of the grinding process (solid lines). The calculated patterns from single crystal structures (dotted lines) are reported as a reference for the identification of the phases, with the characteristic peaks of the triclinic co-crystal highlighted in yellow. The red rectangle evidences the appearance of CC-T.

## 7. Effect of the CC-T form on the concentration profiles in LAG condition

Of the four LAG experiments, the two tests with lower water content (HW30 and LW10) showed the presence of the CC-T form in the reagents profiles (Figure ESI 10, Figure ESI 12) and slower kinetics (green and purple line in Figure ESI 15b respectively), suggesting that the appearance of the triclinic form influences the concentration profile and can be appreciated even if the rapidity of the formation doesn't allow for the complete separation of the intermediate in its own component. To investigate if the change observed in the concentration profile can be related to the presence of the triclinic form, the experimental patterns for the HW30 and LW10 tests, measured at selected times, are compared in Figure ESI 15a. The appearance (black line), the maximum presence (blue line), and the disappearance (red line) of CC-T can be appreciated from the marked intensity variation of the characteristic peaks, highlighted in yellow. The large black, blue and red dots in figure Figure ESI 15b correlate the PXRD patterns with the respective data point on the kinetics. It can be observed that the large blue dots correspond for both HW30 and LW10 experiments to the last data acquisition before the drop of the profile, while the large red dots are at the bottom of the curve. Therefore, the descending section of the curve correctly represents the disappearance not only of the reagents, but also of CC-T. The formation of CC-T, on the contrary, cannot be appreciated with the 2-component model, since its signal is combined with the reagents present from the beginning, but the patterns confirm that it is an extremely rapid process: the CC-T phase reaches its maximum after 80 s of grinding in the 25 Hz test, and after only 20 s in the 50Hz test.

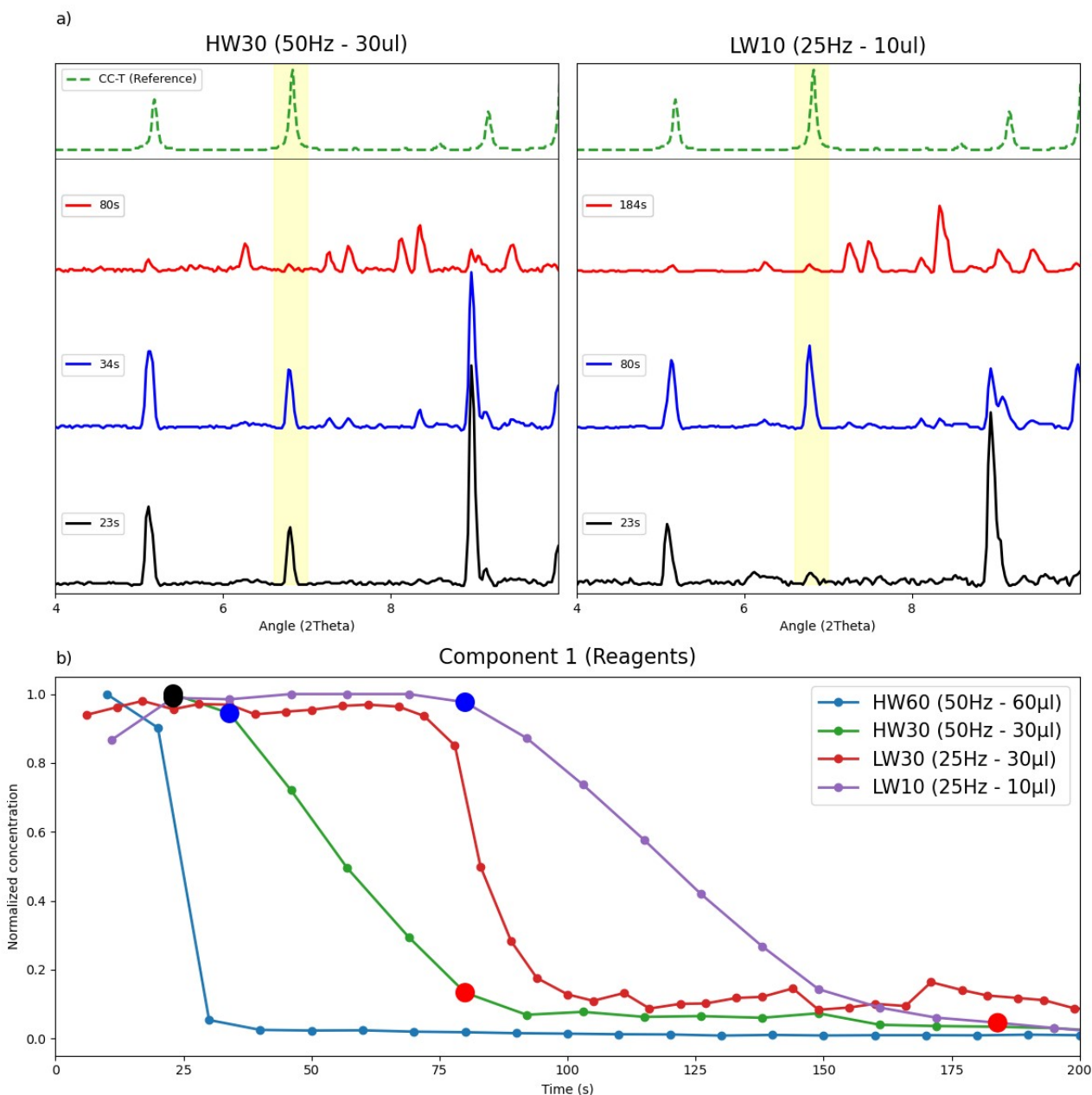


Figure ESI 15 - a) Experimental patterns of the HW30 and LW10 test at selected time points corresponding to the appearance (black line), the maximum presence (blue line), and the disappearance (red line) of the triclinic co-crystal polymorph; with dotted lines are reported the calculated patterns from the single crystal structures as reference. b) Normalized concentration profiles of the reagents component obtained by the MCR-ALS calculation for the LAG experiments data. The big black, blue, and red dots correlate, with matching colours, the patterns shown in graph "a" with the position on the respective curves.